NASA/TP–2007–214751

Comparison of the Exclusion Volume and Probability Threshold Methods for Debris Avoidance for the STS Orbiter and International Space Station

J. L. Foster, Jr., Ph.D.
Barrios Technology, Ltd.

J. H. Frisbee, Jr.
United Space Alliance, LLC

This document was originally written in October of 1999.

May 2007

THE NASA STI PROGRAM OFFICE . . . IN PROFILE

Since its founding, NASA has been dedicated to the advancement of aeronautics and space science. The NASA Scientific and Technical Information (STI) Program Office plays a key part in helping NASA maintain this important role.

The NASA STI Program Office is operated by Langley Research Center, the lead center for NASA's scientific and technical information. The NASA STI Program Office provides access to the NASA STI Database, the largest collection of aeronautical and space science STI in the world. The Program Office is also NASA's institutional mechanism for disseminating the results of its research and development activities. These results are published by NASA in the NASA STI Report Series, which includes the following report types:

- TECHNICAL PUBLICATION. Reports of completed research or a major significant phase of research that present the results of NASA programs and include extensive data or theoretical analysis. Includes compilations of significant scientific and technical data and information deemed to be of continuing reference value. NASA's counterpart of peer-reviewed formal professional papers but has less stringent limitations on manuscript length and extent of graphic presentations.

- TECHNICAL MEMORANDUM. Scientific and technical findings that are preliminary or of specialized interest, e.g., quick release reports, working papers, and bibliographies that contain minimal annotation. Does not contain extensive analysis.

- CONTRACTOR REPORT. Scientific and technical findings by NASA-sponsored contractors and grantees.

- CONFERENCE PUBLICATION. Collected papers from scientific and technical conferences, symposia, seminars, or other meetings sponsored or cosponsored by NASA.

- SPECIAL PUBLICATION. Scientific, technical, or historical information from NASA programs, projects, and mission, often concerned with subjects having substantial public interest.

- TECHNICAL TRANSLATION. English-language translations of foreign scientific and technical material pertinent to NASA's mission.

Specialized services that complement the STI Program Office's diverse offerings include creating custom thesauri, building customized databases, organizing and publishing research results . . . even providing videos.

For more information about the NASA STI Program Office, see the following:

- Access the NASA STI Program Home Page at http://www.sti.nasa.gov

- E-mail your question via the internet to help@sti.nasa.gov

- Fax your question to the NASA Access Help Desk at (301) 621-0134

- Telephone the NASA Access Help Desk at (301) 621-0390

- Write to:
  NASA Access Help Desk
  NASA Center for AeroSpace Information
  7121 Standard
  Hanover, MD 21076-1320

NASA/TP–2007–214751

Comparison of the Exclusion Volume and Probability Threshold Methods for Debris Avoidance for the STS Orbiter and International Space Station

J. L. Foster, Jr., Ph.D.
Barrios Technology, Ltd.

J. H. Frisbee, Jr.
United Space Alliance, LLC

This document was originally written in October of 1999.

National Aeronautics and
Space Administration

Lyndon B. Johnson Space Center
Houston, Texas 77058

May 2007

Available from:

NASA Center for AeroSpace Information
7121 Standard Drive
Hanover, MD 21076-1320
301-621-0390

National Technical Information Service
5285 Port Royal Road
Springfield, VA 22161
703-605-6000

This report is also available in electronic form at http://ston.jsc.nasa.gov/collections/TRS/

TABLE OF CONTENTS

1.0 Introduction 1
2.0 STS State Vector Covariances 1
3.0 Debris and ISS State Vector Covariance 3
4.0 Collision Probability 4
5.0 Maneuver Rate and Risk Reduction 4
6.0 Exclusion Volume Results 6
7.0 Threshold Method Results 9
8.0 Discussion 13
9.0 References 14
Appendix A. Correlation Coefficients and Normality of STS Covariance 15
Appendix B. Accuracy Bins for November 1998 Orbital Debris Population 17
Appendix C. Relative Angle Coefficients 17
Appendix D. STS Orbiter Area 18
Appendix E. Useful Mathematics in the Integral Evaluations 19

TABLES

Table 1. Standard Deviations of the Diagonal Position Terms-Covariance Matrices, *C*..... 2

Table 2. Debris and ISS scale factors from Reference 7..... 3

Table 3. Debris scale factor table for this work 3

Table 4. Fractional Residual Risk Versus Annual Maneuvers for 2-hour Propagation..... 7

Table 5. Fractional Residual Risk Versus Annual Maneuvers for 4-hour Propagation..... 8

Table 6. Fractional Residual Risk Versus Annual Maneuvers for 8-hour Propagation..... 8

Table 7. Fractional Residual Risk Versus Annual Maneuvers for 24 and 48-Hour State Vector Propagation. 9

Table A1. Correlation Coefficients for STS State Vector Covariance for 4-hour State Vector Propagation from Epoch..... 15

Table B1. The Flux and EDR Associated With Each Accuracy Bin 17

Table C1. Distribution of Relative Angle Coefficients for 9/6/97 LEO Debris Catalog..... 17

FIGURES

Figure 1. Fractional residual risk for STS for 2 hours between epoch and time of conjunction. 10

Figure 2. Fractional residual risk for STS for 4 hours between epoch and time of conjunction. 10

Figure 3. Fractional residual risk for STS for 8 hours between epoch and time of conjunction. 11

Figure 4. Fractional residual risk for ISS for 8 hours between epoch and time of conjunction... 12

Figure 5. Fractional residual risk for ISS for 24 hours between epoch and time of conjunction. 12

Figure 6. Comparison of threshold method results for ISS for 8, 24, and 48 hours between epoch and time of conjunction. 13

Figure A1. Quantile - Quantile Plots showing a comparison of 4-hour propagated STS data, indicated by the data points, against $N(0,\sigma)$ distributions indicated by the straight lines. 16

Acronyms

ISS	International Space Station
LEO	low Earth orbit
SP	special perturbations
STS	Space Transportation System

1.0 INTRODUCTION

Both the "exclusion volume" (Reference 1) and "maneuver threshold" (Reference 2) methods have been carefully investigated by performing detailed calculations of debris risk over time and debris avoidance maneuver rate for the Space Transportation System (STS) Orbiter and the International Space Station (ISS). The exclusion volume and the threshold methods are inseparably related. The underlying mathematics of the two methods is identical. Also, conjunction screening is based upon an exclusion volume; the efficiency of the screening exclusion volume is the limiting efficiency of the debris avoidance process, whether the threshold method or the exclusion box method is employed in the final decision process. This analysis shows the threshold method to have the advantages of somewhat better risk reduction and far fewer maneuvers.

All computations are based on empirically determined covariance distributions for STS and the orbital debris population. The covariance of the ISS is assumed to be that of an orbital debris object, subject to the same atmospheric drag as the ISS. State vector covariances for STS were determined from recent tracking data for 2, 4, 8, and 12-hour propagation times (Reference 3) for low, moderate, and high vehicle activity. These covariances were combined with the debris covariances determined in Reference 4, to determine the maneuver rate and fractional residual risk associated with different screening box shapes and sizes and different collision probability maneuver thresholds.

The exclusion volume calculations, performed here, supersede all previous calculations. In Reference 5, the ratio of the exclusion volume to the volume of an ellipsoidal surface with a constant collision probability, equal to that of a maneuver threshold, was calculated. That ratio weighted over the distribution of debris position uncertainty, was taken to be the exclusion volume efficiency. The exclusion volume calculations in this work, again weighted over the distribution of debris and space vehicle uncertainty, are mathematically precise.

In Section I the STS covariance data are discussed, while in Section II the results of the debris covariance distribution determined in Reference 1 is presented. The expression for the collision probability is given in section III. The exclusion volume and threshold methods are explained in Section IV and their interrelation is shown. The exclusion volume method is applied to both ISS and STS in section V. The threshold method is applied in Section VI. Section VII contains a general discussion of results.

2.0 STS STATE VECTOR COVARIANCES

Post Flight Attitude and Trajectory History ephemeris data from flights STS82, STS85, STS87, STS88, STS90 and STS92 were analyzed to provide a covariance matrix for low, moderate and high vehicle activity, for propagation times from epoch of 2, 4, 8, and 12 hours. The 6x6 covariance matrix was calculated from the state vector deviations from prediction ΔS as

$$C = \frac{1}{N}\sum_{1}^{N} \Delta S^T \Delta S \tag{1}$$

where ΔS is $\left[\Delta U \;\; \Delta V \;\; \Delta W \;\; \Delta \dot{U} \;\; \Delta \dot{V} \;\; \Delta \dot{W}\right]$ and N is the vertical dimension of ΔS corresponding to the number of samples for a given activity and propagation time. Table 1 shows the standard

deviations, $\sigma_i = \sqrt{C_{i,i}}$, of the diagonal position terms of the covariance matrices, *C*. Appendix A shows covariances and normality plots for a 4-hour state vector propagation.

The effects of atmospheric drag, vents, attitude maneuvers and translation maneuvers are implicitly included in these empirical results. Low activity is defined as no attitude maneuvers, moderate activity is less than one attitude maneuver per orbit, and high activity is more than one attitude maneuver per orbit. The results here presented represent a realistic estimate of the actual propagated covariances. A very large number of STS orientations and jet firing combinations are possible. Because of a scarcity of data for any given combination, the numbers represent averages with the appropriate level of activity. The 2-hour propagation approximates the minimum possible time between epochs and conjunction for which a debris avoidance maneuver might be performed while the 4-hour propagation approximates the longest time interval for which one might be sure enough of the STS Orbiter vector for a maneuver decision to be appropriate.

Table 1. Standard Deviations of the Diagonal Position Terms-Covariance Matrices, *C*

2-Hour Propagation					
	Samples	Duty	Low Activity	Medium Activity	High Activity σ
σU (m)	95	77%	55.4	76.2	125.7
σV (m)	13	10%	273.0	680.2	981.2
σW (m)	16	13%	84.3	92.3	139.2
4-Hour Propagation					
σU (m)	91	75%	66.7	92.6	110.4
σV (m)	13	11%	540.6	1412.0	1970.6
σW (m)	18	15%	86.6	110.5	171.6
8-Hour Propagation					
σU (m)	93	76%	124.8	264.2	285.3
σV (m)	13	11%	1530	4789	6038
σW (m)	17	14%	116.5	75.0	175.2
12-Hour Propagation					
σU (m)	60	79%	135.3	287.2	478.7
σV (m)	7	9%	2328	7558	12030
σW (m)	9	12%	107.2	123.1	160.5

3.0 DEBRIS AND ISS STATE VECTOR COVARIANCE

Reference 4, ISS Debris Avoidance Maneuver Threshold Analysis, documents a regression analysis employing data from Reference 6, Space Station Debris Avoidance Final Report, from which an orbital position covariance is statistically determined for an 8-hour state vector propagation as a function of number of observation tracks per day and the drag-induced energy dissipation rate per unit mass, for the debris object. This permitted the separate determination of an 8-hour propagated covariance for each of the 288 low earth orbit (LEO) objects and each of the 432 deep space objects crossing the 400 ±40 km altitude band. The objects were sorted by downtrack uncertainty, separated into 15 uncertainty bins, with the flux weighted average uncertainty determined for each bin. It was felt that the 15 bins provided sufficiently low granularity to represent the entire LEO population with reasonable accuracy while the use of only 15 bins allowed detailed calculations for each bin. The resulting 15 characteristic accuracy bins are described in Appendix B. The angular direction of the debris population, as seen from a space vehicle, relative to its velocity vector, for a 51.5-degree inclination orbit is shown in Appendix C.

Scaling (Reference 7) was performed to establish a 24-hour propagation covariance by taking the ratios of the limited amount of 24-hour propagation σ_U, σ_V, and σ_W values to those for 8 hours. In this work, the same process is performed for zero propagation time (epoch). There were no 48-hour data in Reference 7 and a linear extrapolation of 8 and 24 hours was used for 48 hours. The scaling factors are shown in Table 2.

Table 2. Debris and ISS scale factors from Reference 7

	σ_U factor	σ_V factor	σ_W factor
Epoch (0 prop time)	0.75	0.41	1.0
8-hr prop time	1	1	1
24-hr prop time	2.0	3.0	1.5
48-hr prop time	3.5	6.0	2.25

For the 2-hour and 4-hour propagation of the debris covariance, a linear extrapolation,

$$\sigma\ factor = \frac{\sigma_{8hr}\ factor - \sigma_{epoch}\ factor}{8} t + \sigma_{epoch}\ factor \quad , \qquad (2)$$

between the 0 and 8-hour values was employed. A similar linear extrapolation was performed between 8 and 24 hours for the 12-hour data. Table 3 displays the extrapolated values for 0, 2, 4, 6, 8, and 12 hours of propagation.

Table 3. Debris scale factor table for this work

Prop time (hrs)	σ_U factor	σ_V factor	σ_W factor
0	0.75	0.41	1
2	0.813	0.558	1
4	0.875	0.705	1
6	0.938	0.853	1
8	1	1	1
12	1.25	1.50	1.12

The correlation between the radial and down track position uncertainties was not measured in Reference 4., and was set to zero in this work. A reasonable trial value of -0.5 did not substantively alter any result.

The ISS state vector uncertainty was taken to be that of the current ISS configuration, calculated by the algorithm that produced the data in Appendix B. The drag and calculated covariance is close to that of bin 3 in Table A.1.

4.0 COLLISION PROBABILITY

In this section, the maneuver rate and risk reduction associated with each of the 15 satellite groups is determined, using the method of Reference 1, for a complete range of possible maneuver thresholds. The equations were modified to allow inclusion of the UV correlation coefficients. Use of UV correlation coefficients of -0.5 made negligible difference in the results. The UV correlation coefficients were not used because of complications that would arise in maneuver box determination in Section IV. The results for each of the 15 groups are combined to produce a total maneuver rate and an aggregate residual risk.

For the purposes of this work, we assume the debris conjunctor and the target vehicle travel parallel to the surface of the earth with the same velocity, and with known state vector uncertainties, which we express in terms of covariance matrices.

The spatial part of the covariance matrix for the space vehicle and debris conjunctor is taken to be of the form

$$C_{UVW}^{SV} = \begin{bmatrix} \sigma_{UU}^{SV} & \sigma_{UV}^{Sv} & 0 \\ \sigma_{VU}^{Sv} & \sigma_{VV}^{SV} & 0 \\ 0 & 0 & \sigma_{WW}^{SV} \end{bmatrix} \quad \text{and} \quad C_{UVW}^{deb} = \begin{bmatrix} \sigma_{UU}^{deb} & \sigma_{UV}^{deb} & 0 \\ \sigma_{VU}^{deb} & \sigma_{VV}^{deb} & 0 \\ 0 & 0 & \sigma_{WW}^{deb} \end{bmatrix} \text{, where}$$

Representing the target object as a sphere of radius R, for the conjuncting object at position x_0, y_0 relative to the space vehicle at time of conjunction, the collision probability is

$$P(r < R) = \frac{1}{2\pi\,\lambda 1\,\lambda 2} \int_{-R}^{R} \int_{-\sqrt{x^2-R^2}}^{\sqrt{x^2-R^2}} e^{-\frac{(x-x_0)^2}{2\lambda 1^2}} e^{-\frac{(y-y_0)^2}{2\lambda 2^2}} dxdy \quad , \tag{3}$$

where $\lambda 1^2(\theta)$, $\lambda 2^2(\theta)$ are the non-zero elements of the diagonalized projection of $C_{inertial}^{SV}$ + $C_{inertial}^{deb}$ on to the conjunction plane and θ is the angle between the vehicle velocity vector and that of the debris object (Reference 8).

5.0 MANEUVER RATE AND RISK REDUCTION

We first consider the implications of an exclusion volume in the shape of a hockey puck of height 2h and diameter 2L, in the plane defined by the debris and space vehicle velocity vectors. This figure presents a constant area in the collision plane independent of the direction from which the debris is coming. The annual risk to the space vehicle from debris objects penetrating the puck is

$$Ar = \sum_j flux_j \sum_i D(\phi_i) \frac{1}{2\pi \lambda 1_{i,j} \lambda 2_{i,j}} \int_{-L}^{L} \int_{-h}^{h} \int_{-R}^{R} \int_{-\sqrt{R^2-x^2}}^{\sqrt{R^2-x^2}} e^{-\frac{(x-\eta)^2}{2\lambda 1_{i,j}^2} - \frac{(x-\zeta)^2}{2\lambda 2_{i,j}^2}} dy\, dx\, d\eta\, d\zeta \tag{4}$$

where $flux_j$ is the flux associated with the jth flux accuracy bin and $D(\phi_i)$ is the fraction of the total flux coming from a 15-degree angular region about direction ϕ_i. Here R is the radius of a sphere encompassing the space vehicle, 23 m for STS and 60 m for the assembly-complete ISS. For both the assembly-complete ISS and the STS, the area of the cross section of the sphere is 5 times the projected area of the space vehicle. *Ar* depends strongly on the vehicle size. The fractional residual risk, *Frr*, defined as

$$Frr = 1 - \frac{Ar}{\pi R^2 F_T} \tag{5}$$

where F_T is the total flux, has negligible dependence on vehicle size as long as L >> R and h >> R and has no dependence at all on total debris flux. If the exclusion volume is a box, rather than a puck, *L* and *h* become dependent on direction, i.e. L_i and h_i. If the cross section of the exclusion volume is elliptical rather than square, then

$$L_i = a_i \sqrt{1 - h_i / b_i} \tag{6}$$

where a_i and b_i are the semimajor and semiminor axes for the elliptical cross section.

The exclusion volume method uses a single exclusion volume, independent of state vector accuracy. In the maneuver threshold method, the exclusion region is defined by the surface of constant collision probability corresponding to the maneuver threshold.

For debris from a given direction, the curves of constant collision probability are the intercept of the collision plane and the surfaces of constant collision probability. The curves of constant collision probability in the collision plane are approximately ellipses. Thus for each of our 15 accuracy bins there will be a different ellipse for each incident debris direction. The fractional residual risk becomes

$$Frr = 1 - \frac{1}{\pi R^2 F_T} \sum_j flux_j \sum_i D(\phi_i) \frac{1}{2\pi \lambda 1_{i,j} \lambda 2_{i,j}} \int_{-b_{i,j}}^{b_{i,j}} \int_{-a_{i,j}\sqrt{1-\frac{\zeta^2}{b_{i,j}}}}^{a_{i,j}\sqrt{1-\frac{\zeta^2}{b_{i,j}}}} \int_{-R}^{R} \int_{-\sqrt{R^2-x^2}}^{\sqrt{R^2-x^2}} e^{-\frac{(x-\eta)^2}{2\lambda 1_{i,j}^2} - \frac{(x-\zeta)^2}{2\lambda 2_{i,j}^2}} dy\, dx\, d\eta\, d\zeta \tag{7}$$

The integral in equation 3 can be reduced to a one-dimensional numeric integral in terms of the error function. Though computing the collision probability by multiplying the probability density function by the vehicle area, rather then by carrying out the integral, often results in orders of magnitude errors in the collision probability, it was observed in this work that the integrals over

the vehicle area in equations 4 and 7 could be replaced by the probability density times the vehicle area with a resultant error of less than a tenth of one percent. The integral in equation 4 is then calculable in closed form while the integral in equation 7 reduces to a one-dimensional numeric integral (Appendix E).

For exclusion volumes with rectangular cross sections and constant height 2h, the annual maneuver rate is given by

$$M = \sum_j flux_j \sum_i D(\phi_i) \int_{-L_i}^{L_i} \int_{-h}^{h} d\eta\, d\zeta \qquad . \tag{8}$$

For exclusion volumes with an elliptical cross section, the annual maneuver rate is given by

$$M = \sum_j flux_j \sum_i D(\phi_i) \int_{-b_{i,j}}^{b_{i,j}} \int_{-a_{i,j}\sqrt{1-\frac{\zeta^2}{b_{i,j}}}}^{a_{i,j}\sqrt{1-\frac{\zeta^2}{b_{i,j}}}} d\eta\, d\zeta \qquad , \tag{9}$$

where $a_{i,j}$ and $b_{i,j}$ are the semimajor and semiminor axes of the ellipse.

6.0 EXCLUSION VOLUME RESULTS

Maneuver rate and fractional residual risk were calculated for a variety of exclusion volumes. The efficacy of the 1 km radius sphere proposed by the Russian, and that of boxes ±1x3x1 km, ±2x5x2 km, ±3x10x32 km, and ±5x25x5 km was determined for propagation times of 2, 4, 8, 24, and 48 hours. The effectiveness of optimized pucks having the same and different maneuver rates as was also investigated. For a given maneuver rate, the optimized puck, optimized box, and optimized ellipsoid had the same fractional residual risk.

Tables 4, 5, and 6 show the results for propagation times of 2, 4, and 8 hours for ISS and for STS in high and low activity modes.

Table 4. Fractional Residual Risk Versus Annual Maneuvers for 2-hour Propagation

	Fractional Residual Risk				
Exclusion volume	ISS	STS low	STS med	STS high	Annual maneuvers
1 km radius sphere	0.28	0.025	0.30	0.36	0.83
±0.36x2.2 km puck	0.21	0.21	0.21	0.23	0.83
±1x3x1 km box	0.20	0.20	0.20	0.22	1.8
±0.43x4 km puck	0.17	0.17	0.18	0.18	1.8
±0.67x4.5 km puck	0.15	0.15	0.15	0.15	3.2
±2x5x2 km box	0.15	0.14	0.15	0.15	6.9
±1x6.5 km puck	0.14	0.13	0.13	0.14	6.9
±3x10x3 km box	0.12	0.12	0.12	0.12	17
±1.6x10 km puck	0.11	0.11	0.11	0.11	17
±5x25x5 box	0.105	0.104	0.105	0.105	49
±2.3x20 km puck	0.095	0.095	0.095	0.095	49
±5x25 km puck	0.08	0.08	0.08	0.08	132
±5x40 km puck	0.07	0.07	0.07	0.07	212

Table 5. Fractional Residual Risk Versus Annual Maneuvers for 4-hour Propagation

	Fractional residual risk				
Exclusion volume	ISS	STS low	STS med	STS high	Annual maneuvers
1 km radius sphere	0.33	0.3	0.47	0.56	0.83
±0.36x2.2 km puck	0.22	0.23	0.27	0.33	0.83
±1x3x1 km box	0.23	0.22	0.23	0.39	1.8
±0.43x4 km puck	0.19	0.19	0.19	0.20	1.8
±0.67x4.5 km puck	0.16	0.16	0.16	0.17	3.2
±2x5x2 km box	0.16	0.16	0.17	0.17	6.9
±1x6.5 km puck	0.13	0.14	0.14	0.14	6.9
±3x10x3 km box	0.13	0.13	0.14	0.14	17
±1.6x10 km puck	0.12	0.12	0.12	0.12	17
±5x25x5 box	0.11	0.11	0.11	0.11	49
±2.3x20 km puck	0.10	0.10	0.10	0.10	49
±5x25 km puck	0.09	0.09	0.09	0.09	132
±5x40 km puck	0.08	0.08	0.08	0.08	212

Table 6. Fractional Residual Risk Versus Annual Maneuvers for 8-hour Propagation.

	Fractional Residual Risk				
Exclusion volume	ISS	STS low	STS med	STS high	Annual maneuvers
1 km radius sphere	0.43	0.52	0.79	0.83	0.83
±0.36x2.2km puck	0.25	0.31	0.66	0.73	0.83
±1x3x1 km box	0.29	0.35	0.67	0.73	1.8
±0.43x4 km puck	0.21	0.22	0.45	0.53	1.8
±0.67x4.5 km puck	0.18	0.18	0.34	0.41	3.2
±2x5x2 km box	0.19	0.20	0.44	0.52	6.9
±1x6.5 km puck	0.15	0.15	0.22	0.27	6.9
±3x10x3 km box	0.15	0.16	0.27	0.34	17
±1.6x10 km puck	0.13	0.13	0.13	0.13	17
±5x25x5 box	0.12	0.12	0.15	0.18	49
±2.3x20 km puck	0.11	0.11	0.11	0.11	49
±5x25 km puck	0.09	0.09	0.09	0.09	132
±5x40 km puck	0.08	0.08	0.08	0.08	212

Table 7 shows the ISS results for 24 and 48-hour propagation from epoch.

Table 7. Fractional Residual Risk Versus Annual Maneuvers for 24 and 48-Hour State Vector Propagation.

	Fractional Residual Risk		
Exclusion volume	24 hr ISS	48 hr ISS	Annual maneuvers
1 km radius sphere	0.76	0.88	0.83
±1x3x1 km box	0.64	0.81	1.8
±0.43x4 km puck	0.4	0.67	1.8
±0.67x4.5 km puck	0.34	0.57	3.2
±2x5x2 km box	0.41	0.64	6.9
±1x6.5 km puck	0.26	0.43	6.9
±3x10x3 km box	0.28	0.49	17
±1.6x10 km puck	0.19	0.31	17
±5x25x5 box	0.2	0.33	49
±2.3x20 km puck	0.15	0.20	49
±5x25 km puck	0.13	0.17	132
±4x32 km puck	0.12	0.16	132
±5x40 km puck	0.12	0.14	212

In all cases, the optimized puck is better than the "standard" boxes in current use. The current ±5x25x5 km screening box is especially poor. A ±1.6x10 km puck has a better efficiency for long propagation times with one-third the associated "maneuver" rate.

The pucks should be considered as optimized volumes from which only negligible improvement can be made. Ellipsoids, elongated pucks, round pucks and boxes were extensively investigated. While the optimal exclusion volume is the ellipsoid, the differences between optimized ellipsoids, pucks and boxes were negligible. A box with the same efficiency and maneuver rate can be found by keeping the puck height, multiplying the puck area, A_p, by 0.95, and having the width be 90% of the length of the box.

$$0.95\, A_p = 0.9\, L^2 \quad . \tag{8}$$

7.0 THRESHOLD METHOD RESULTS

Figures 1, 2, and 3 show Fractional Residual Risk as a function of a Annual Maneuver Rate for state vector propagation times of 2, 4, and 8 hours. The line curves depict threshold method results for STS for low, medium, and high vehicle activity levels. The isolated points represent exclusion volume results. Exclusion volumes consisting of a 1 km radius sphere, ±1x3x1 km and ±2x5x2 km boxes and optimized pucks are shown. In the following graphs. P_m is the collision probability threshold for which a maneuver will be performed.

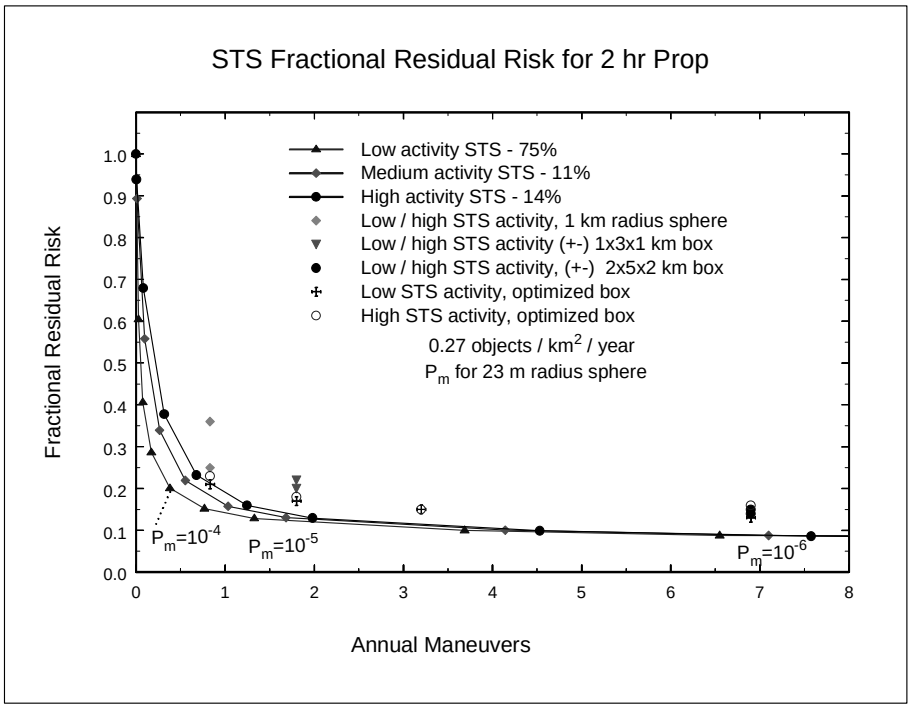

Figure 1. Fractional residual risk for STS for 2 hours between epoch and time of conjunction.

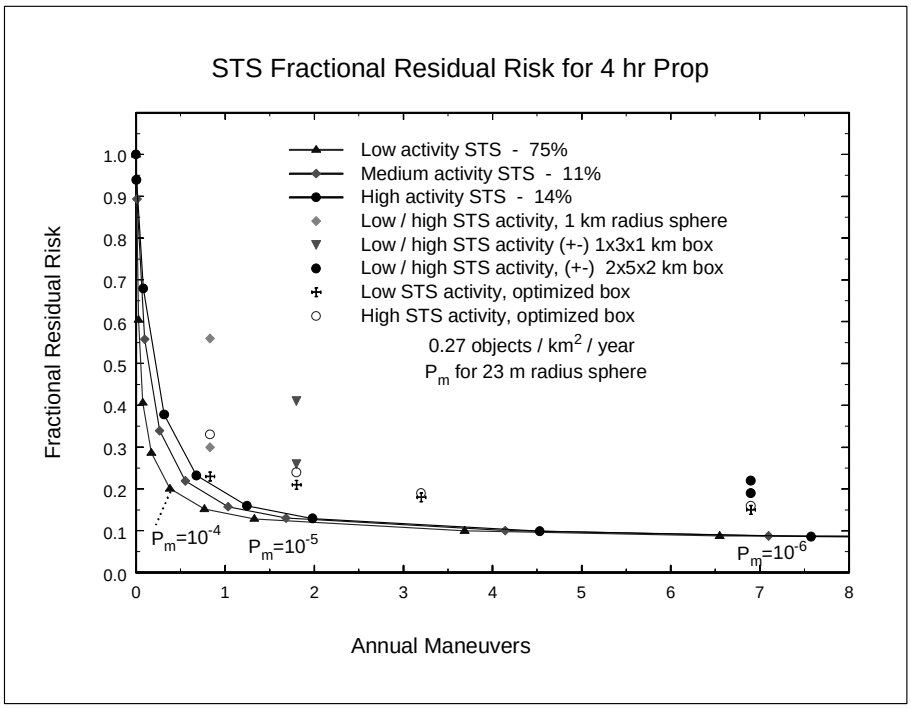

Figure 2. Fractional residual risk for STS for 4 hours between epoch and time of conjunction.

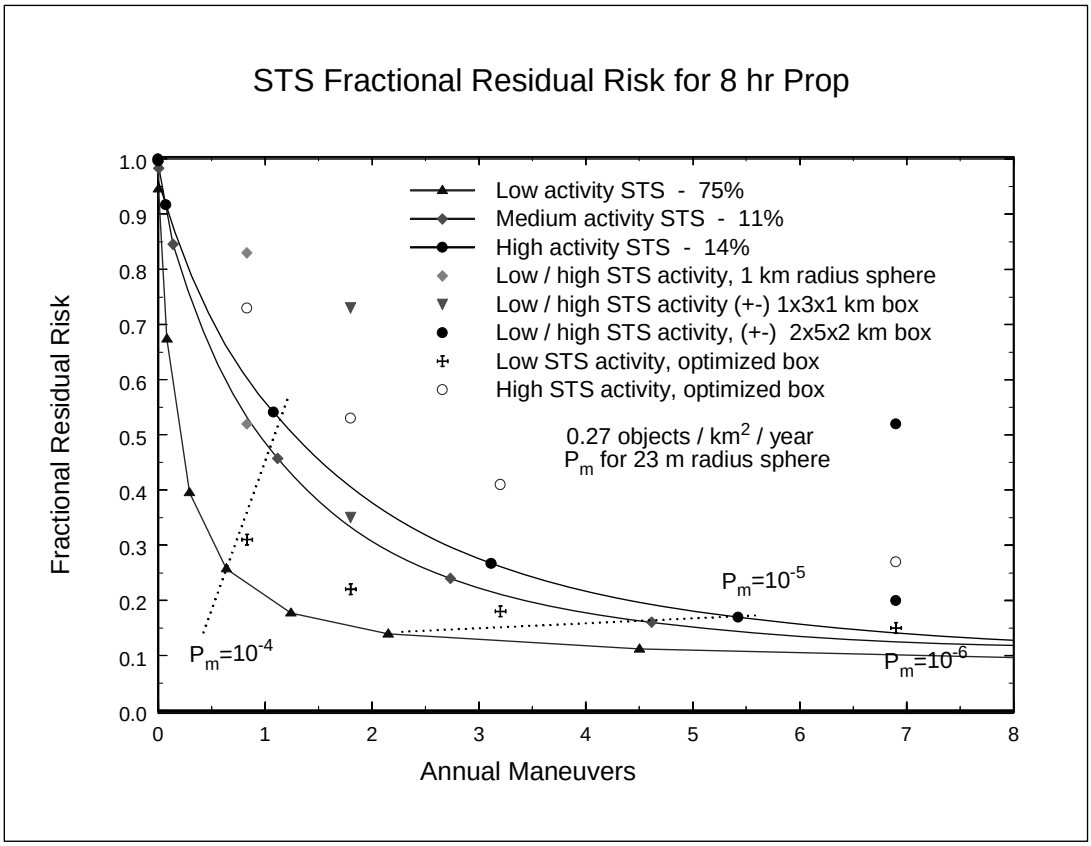

Figure 3. Fractional residual risk for STS for 8 hours between epoch and time of conjunction.

Figures 4 and 5 show ISS fractional residual risk as a function of maneuver rate for state vector propagation times of 8 and 24 hours. The line curve indicates the threshold method results while the isolated points show exclusion volume results.

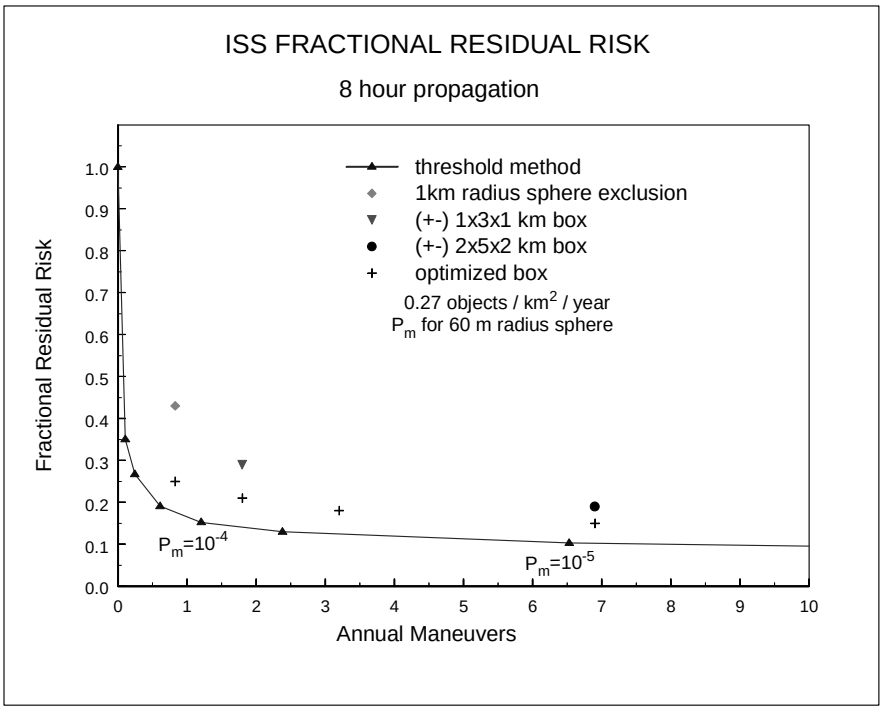

Figure 4. Fractional residual risk for ISS for 8 hours between epoch and time of conjunction.

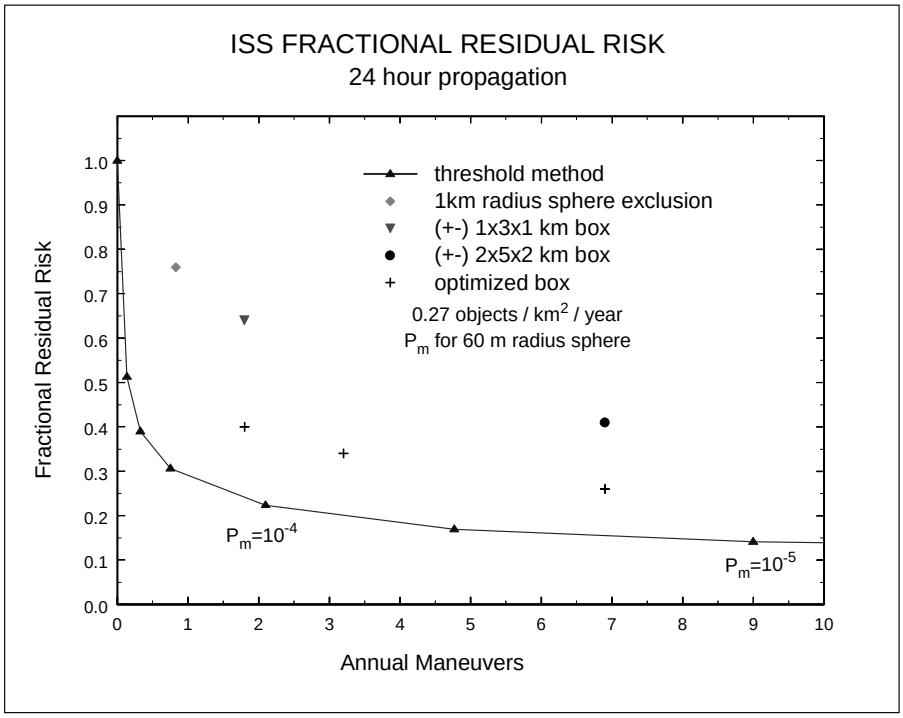

Figure 5. Fractional residual risk for ISS for 24 hours between epoch and time of conjunction.

Figure 6 shows a comparison between 8, 24, and 48-hour propagation ISS threshold results.

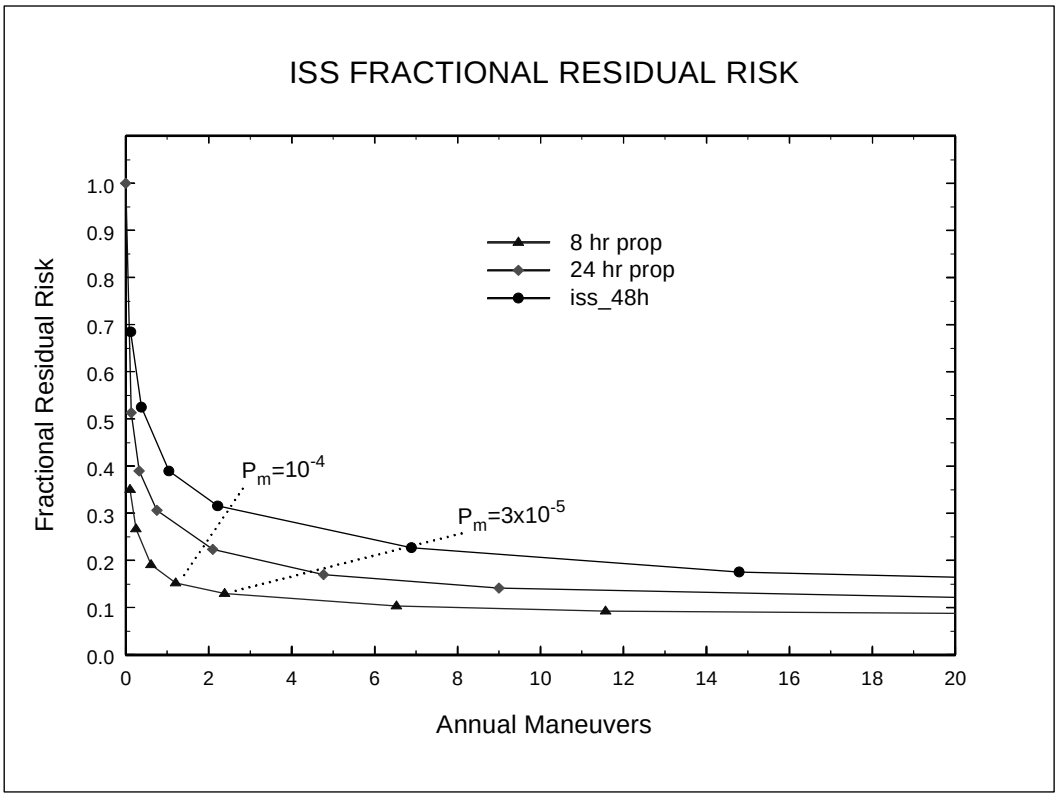

Figure 6. Comparison of threshold method results for ISS for 8, 24, and 48 hours between epoch and time of conjunction.

8.0 DISCUSSION

Results are valid only for U.S. Space Command special-perturbations (SP) processing. The study (Reference 6) was carried out with the high accuracy SP processing and track weighting within standard fit intervals. The exclusion volume results are not applicable to general-perturbations (GP) processed data, or to data fit over an interval so long that model error is apparent in the fit residuals.

Optimized volumes are approximately ellipsoids, which can be very well represented by a round puck. Elongating the puck produces minimal improvement. There always exists a box equivalent. The efficiency of the exclusion volume varies quite slowly with change in dimensions as long as the maneuver rate is kept constant.

A ±0.67x4.5 km puck, with 3.2 maneuvers per year on orbit, has approximately the same efficiency as the famed ±2x5x2 km box with 6.9 maneuvers. The ±0.67x4.5 km puck is interesting as an exclusion volume alternative to the threshold method for low vehicle activity STS and ISS with propagation times of 8 hours or less.

The 10^{-4} red threshold for ISS appears to be high for the smaller STS. A threshold value of $3x10^{-5}$, for 8 hours or less propagation, appreciably reduces residual risk while the maneuver rate remains sustainable.

The overall effectiveness of the debris avoidance process depends upon the screening efficiency. It is vital that dangerous conjunctions be anticipated with sufficient time to increase tasking on the debris object and obtain a stable state vector. The ±5x25x5 km box is clearly inappropriate as a long propagation time screening volume, and needs to be replaced. A ±2.3x20 km puck has the same associated detection rate and appreciably better efficiency, especially for longer propagation times.

9.0 REFERENCES

1) MOD Internal Note, Haynes, M., June 18, 1989.

2) A Parametric Analysis of Orbital Debris Collision Probability and Maneuver Rate for Space Vehicles, JSC-25898, August 1992.

3) Navigation Covariance Analysis, Johnson Space Center, SFOC Transmittal Form No. NAV-98-4237-111, August 18, 1998.

4) ISS Debris Avoidance Maneuver Threshold Analysis (NASA TP-2007-214752), Johnson Space Center DM33, July 6, 1999.

5) Effectiveness of a Maneuver Box for ISS Debris Avoidance Operations, Johnson Space Center DM33, February 19, 1999.

6) Space Station Debris Avoidance Final Report, Kaman Sciences Corporation, KSPACE97-47, January 31, 1997.

7) Position Error Covariance Matrix Scaling Factors for Early Operational ISS Debris Avoidance, Johnson Space Center DM33, May 29, 1998.

8) Estimate of Maneuver Rate and Residual Risk from Orbital Debris as a Function of Maneuver Collision Probability Threshold for the STS Orbiter, Johnson Space Center, DM33, November 2, 1998.

APPENDIX A. CORRELATION COEFFICIENTS AND NORMALITY OF STS COVARIANCE

Table A1. Correlation Coefficients for STS State Vector Covariance for 4-hour State Vector Propagation from Epoch.

Correlation Matrices for 4-Hour STS State Vector Propagation					
Low Activity STS					
U	V	W	U-dot	V-dot	W-dot
1	-0.429	0.0797	0.415	-0.976	0.084
-0.429	1	0.043	-0.994	0.254	-0.075
0.0797	0.043	1	-0.040	-0.103	-0.269
0.415	-0.994	-0.040	1	-0.234	0.0713
-0.976	0.254	-0.103	-0.234	1	-0.089
0.084	-0.075	-0.269	0.0713	-0.089	1
Medium Activity STS					
1	-0.66	0.129	0.668	-0.934	-0.153
-0.66	1	0.052	-0.998	0.386	0.318
0.129	0.052	1	-0.0556	-0.159	-0.335
0.668	-0.998	-0.056	1	-0.399	-0.284
-0.934	0.386	-0.159	-0.399	1	0.041
-0.153	0.318	-0.335	-0.284	0.041	1
High Activity STS					
1	-0.791	-0.080	0.756	-0.841	-0.0635
-0.791	1	0.373	-0.995	0.443	0.112
-0.080	0.373	1	-0.443	-0.162	-0.0077
0.756	-0.995	-0.443	1	-0.386	-0.079
-0.841	0.443	-0.162	-0.386	1	0.0029
-0.0635	0.112	-0.0077	-0.079	0.0029	1

Deviation from Normality

Figure A1 below compares the STS position observation distribution indicated by the points, for 4-hour state vector propagation from epoch, with the predicted normal statistics indicated by the solid lines. Deviation from normality becomes progressively worse as vehicle activity increases. Were the biases to be subtracted, and outliers removed, the agreement with normality would be much better. Figure A1 shows the distributions as the data will be used.

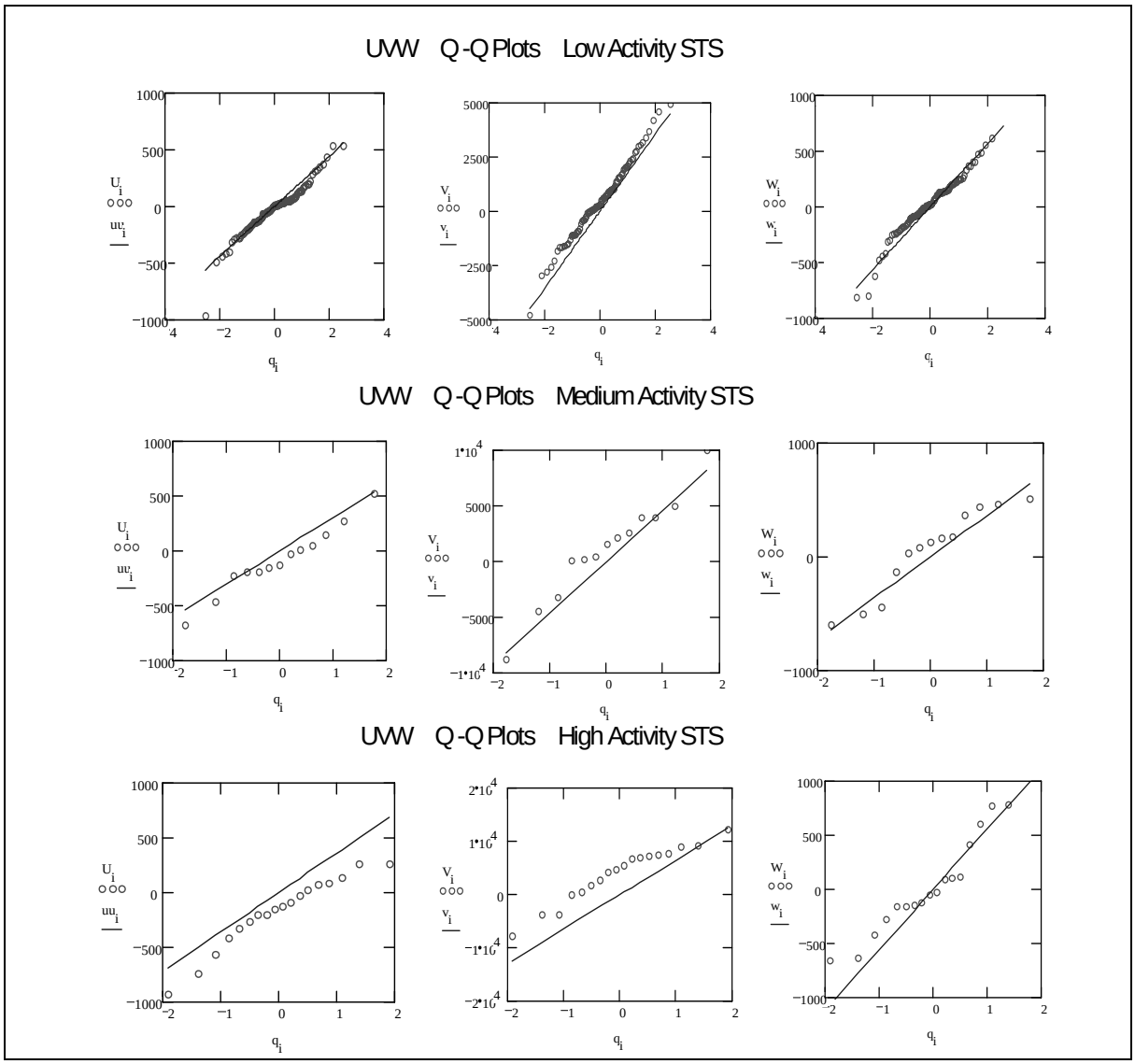

Figure A1. Quantile - Quantile Plots showing a comparison of 4-hour propagated STS data, indicated by the data points, against N(0,σ) distributions indicated by the straight lines.

Here

$q_i = erf^{-1}\{2p_i - 1\}$ where $p_i = \dfrac{i - 0.5}{n}$, with $i = 1$ *to* n, and n = *number of points.*

The $\{U_i\}$, $\{V_i\}$, $\{W_i\}$ are the data points while the $\{uu_i\}$, $\{v_i\}$, and $\{w_i\}$ are $\sqrt{C_{u,u}}\,q_i$, $\sqrt{C_{v,v}}\,q_i$, $\sqrt{C_{w,w}}\,q_i$ respectively. The function $erf(z) = \dfrac{2}{\pi}\int_0^z e^{-t^2}\,dz$ is the error function.

APPENDIX B. ACCURACY BINS FOR NOVEMBER 1998 ORBITAL DEBRIS POPULATION

Table B1. The Flux and EDR Associated With Each Accuracy Bin

Bin	Flux (obj/km^{2}yr)	Av. EDR (watts/kg)
1	0.0117	0.0019
2	0.0406	0.0033
3	0.0161	0.0047
4	0.0275	0.0072
5	0.0170	0.0101
6	0.0285	0.0144
7	0.0176	0.0221
8	0.0238	0.0304
9	0.0063	0.0366
10	0.0120	0.0512
11	0.0234	0.0644
12	0.0077	0.111
13	0.0084	0.220
14	0.0113	0.596
15	0.0230	1.65

$$F_T = \sum_{i=1}^{15} flux_i = 0.275\ obj\ km^{-2}\ year^{-1}$$

APPENDIX C. RELATIVE ANGLE COEFFICIENTS

Table C1. Distribution of Relative Angle Coefficients for 9/6/97 LEO Debris Catalog

Rel. ang.	0°	15°	30°	45°	60°	75°	90°	105°	120°	135°	150°	165°
$D(\phi_j)$	.0000	.0943	.3102	.2295	.2075	.1305	.0238	.0034	.0007	.0001	.0000	.0000

$$\sum D(\phi_j) = 1.0$$

APPENDIX D. STS ORBITER AREA

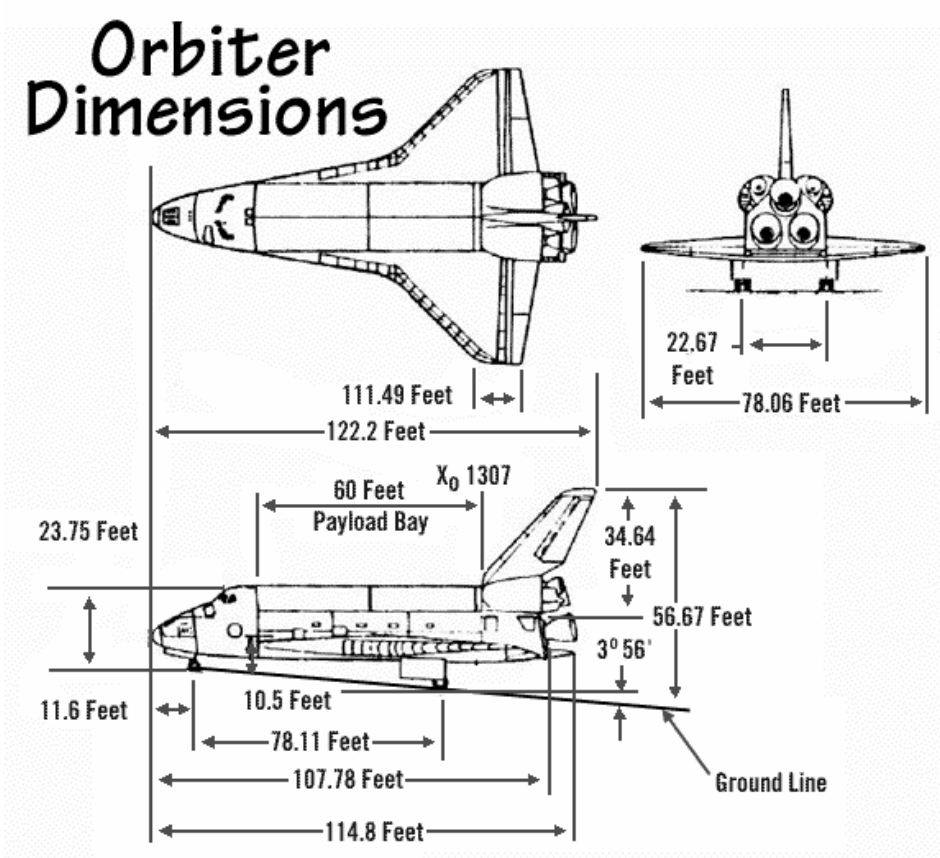

$$frontal\ area = \pi\left(\frac{78.06}{2}\right)\left(\frac{23.75}{2}\right) = 1456.1\ ft^2$$

$$side\ area = \pi\left(\frac{23.75}{2}\right)\left(\frac{114.8}{2}\right) = 2141.4\ ft^2$$

$$top\ area = \pi\left(\frac{78.06}{2}\right)\left(\frac{114.8}{2}\right) = 7038.2\ ft^2$$

$$average\ area = \frac{1456.1 + 2141.4 + 7038.2}{3} = 3245.2\ ft^2 = 330\,m^2$$

represent actual vehicle as 10.3 *meter radius sphere with area* $333 m^2$

The center of mass of the orbiter is required to be from 21.35 to 22.17 meters from the vehicle nose. We represent the orbiter as a 23-meter radius sphere for the collision probability calculation.

APPENDIX E. USEFUL MATHEMATICS IN THE INTEGRAL EVALUATIONS

1. Collision Probability

Equation 3 can be reduced to a single-dimension numeric integral in terms of the error function as shown below.

$$\frac{1}{2\cdot\pi\cdot\sqrt{A\cdot B}}\cdot\int_{-R}^{R} e^{-\frac{(x-a)^2}{2\cdot A}}\cdot\int_{-\sqrt{R^2-x^2}}^{\sqrt{R^2-x^2}} e^{-\frac{(y-b)^2}{2\cdot B}}\,dy\,dx \quad = \tag{E1}$$

$$\frac{1}{4\cdot\sqrt{A}}\cdot\int_{-R}^{R} e^{-\frac{(x-a)^2}{2\cdot A}}\cdot\left(-\operatorname{erf}\left(\frac{-\sqrt{R^2-x^2}+b}{\sqrt{2\cdot B}}\right)+\operatorname{erf}\left(\frac{\sqrt{R^2-x^2}+b}{\sqrt{2\cdot B}}\right)\right)dx$$

The error function, $erf(z)=\frac{2}{\pi}\int_0^z e^{-t^2}dz$, is available in numerous software applications and can be calculated as a series if necessary.

2. Integral over Rectangular Surface

The integral of the 2-dimensional density function over a rectangular area can be written in closed form in terms of the error function.

$$\frac{4}{2\cdot\pi\cdot\sqrt{A\cdot B}}\cdot\int_{0}^{L}\int_{0}^{h} e^{-\frac{x^2}{2\cdot A}}\cdot e^{-\frac{y^2}{2\cdot B}}\,dy\,dx \;=\; \operatorname{erf}\left(\frac{1}{2}\cdot\frac{\sqrt{2}}{\sqrt{B}}\cdot L\right)\cdot\operatorname{erf}\left(\frac{1}{2}\cdot\sqrt{2}\cdot\frac{h}{\sqrt{A}}\right) \tag{E2}$$

3. Reduction of Exact Expression to 2-Dimensional Integral

The integral of the probability of collision with a sphere of radius R over a rectangular area can be reduced from a 4-dimensional to a 2-dimensional integral as shown below.

$$\frac{1}{2\cdot\pi\cdot\sqrt{A\cdot B}}\cdot\int_0^L\int_0^h\int_{-R}^{R}\int_{-\sqrt{R^2-x^2}}^{\sqrt{R^2-x^2}} e^{\frac{(x-\eta)^2}{2\cdot A}}\cdot e^{-\frac{(y-\zeta)^2}{2\cdot B}}\,dy\,dx\,d\eta\,d\zeta \quad = \tag{E3a}$$

$$\frac{4}{2\cdot\pi\cdot\sqrt{A\cdot B}}\cdot\int_{-R}^{R}\int_0^L e^{-\frac{(x-\eta)^2}{2\cdot A}}\,d\eta\cdot\int_{-\sqrt{R^2-x^2}}^{\sqrt{R^2-x^2}}\int_0^h e^{-\frac{(y-\zeta)^2}{2\cdot B}}\,d\zeta\,dy\,dx \quad =$$

$$\int_{-R}^{R}\left[\operatorname{erf}\left[\frac{(L-x)}{\sqrt{2\cdot A}}\right]+\operatorname{erf}\left(\frac{1}{\sqrt{2\cdot A}}\cdot x\right)\right]\cdot\int_{-\sqrt{R^2-x^2}}^{\sqrt{R^2-x^2}}\left[\operatorname{erf}\left[\frac{(h-y)}{\sqrt{2\cdot B}}\right]+\operatorname{erf}\left(\frac{1}{\sqrt{2\cdot B}}\cdot y\right)\right]dy\,dx \tag{E3b}$$

The use of expression E3b permitted numeric solution of the equivalent expression E3a. This allowed verification of the validity of using expression E2 in place of E3. For an ISS-sized vehicle, L>>R and h>>R and the numeric results do not differ significantly. Also, a Taylor expansion of the error function in E3b reduces to E2 plus a correction.

REPORT DOCUMENTATION PAGE

Form Approved
OMB No. 0704-0188

Public reporting burden for this collection of information is estimated to average 1 hour per response, including the time for reviewing instructions, searching existing data sources, gathering and maintaining the data needed, and completing and reviewing the collection of information. Send comments regarding this burden estimate or any other aspect of this collection of information, including suggestions for reducing this burden, to Washington Headquarters Services, Directorate for Information Operations and Reports, 1215 Jefferson Davis Highway, Suite 1204, Arlington, VA 22202-4302, and to the Office of Management and Budget, Paperwork Reduction Project (0704-0188), Washington, DC 20503.

1. AGENCY USE ONLY *(Leave Blank)*	2. REPORT DATE	3. REPORT TYPE AND DATES COVERED
	May 2007	NASA Technical Paper

4. TITLE AND SUBTITLE
Comparison of the Exclusion Volume and Probability Threshold Methods of Debris Avoidance for the STS Orbiter

5. FUNDING NUMBERS

6. AUTHOR(S)
J.L. Foster (Barrios Technology), J.H. Frisbee (United Space Alliance)

7. PERFORMING ORGANIZATION NAME(S) AND ADDRESS(ES)
Lyndon B. Johnson Space Center
Houston, Texas 77058

8. PERFORMING ORGANIZATION REPORT NUMBERS
S-1001

9. SPONSORING/MONITORING AGENCY NAME(S) AND ADDRESS(ES)
National Aeronautics and Space Administration
Washington, DC 20546-0001

10. SPONSORING/MONITORING AGENCY REPORT NUMBER
TP-2007-214751

11. SUPPLEMENTARY NOTES

12a. DISTRIBUTION/AVAILABILITY STATEMENT
Available from the NASA Center for AeroSpace Information (CASI)
7115 Standard
Hanover, MD 21076-1320 Category: 17

12b. DISTRIBUTION CODE

13. ABSTRACT *(Maximum 200 words)*
Both the “exclusion volume” and “maneuver threshold” methods have been carefully investigated by performing detailed calculations of debris risk over time and debris avoidance maneuver rate for the Space Transportation System Orbiter and the International Space Station. The underlying mathematics of the two methods is identical. Also, conjunction screening is based upon an exclusion volume; the efficiency of the screening exclusion volume is the limiting efficiency of the debris avoidance process, whether the threshold method or the exclusion box method is employed in the final decision process. This analysis shows the threshold method to have the advantages of somewhat better risk reduction and far fewer maneuvers.
All computations are based on empirically determined covariance distributions for STS and the orbital debris population. The covariance of the ISS is assumed to be that of an orbital debris object, subject to the same atmospheric drag as the ISS. State vector covariances for STS were determined from recent tracking data for 2, 4, 8, and 12-hour propagation times for low, moderate, and high vehicle activity. These covariances were combined with the debris covariances, to determine the maneuver rate and fractional residual risk associated with different screening box shapes and sizes and different collision probability maneuver thresholds.

14. SUBJECT TERMS	15. NUMBER OF PAGES	16. PRICE CODE
Space debris, obstacle avoidance, Global Tracking Network, space surveillance, exclusion	32	

17. SECURITY CLASSIFICATION OF REPORT	18. SECURITY CLASSIFICATION OF THIS PAGE	19. SECURITY CLASSIFICATION OF ABSTRACT	20. LIMITATION OF ABSTRACT
Unclassified	Unclassified	Unclassified	Unlimited